Microchimica Acta (2021) 188: 217
https://doi.org/10.1007/s00604-021-04859-1

ORIGINAL PAPER

Free-standing electrochemical biosensor for carcinoembryonic antigen detection based on highly stable and flexible conducting polypyrrole nanocomposite

Jingyao Song[1] · He Teng[1] · Zhenying Xu[1] · Nianzu Liu[1] · Liang Xu[1] · Lu Liu[1] · Fengxian Gao[1] · Xiliang Luo[1]

Received: 25 December 2020 / Accepted: 13 May 2021 / Published online: 31 May 2021

Abstract

A flexible free-standing electrochemical biosensor to detect carcinoembryonic antigen (CEA) is described based on a conducting polypyrrole (PPy) nanocomposite film electrode. The conducting PPy composite was constructed by the sandwiched structure formed by PPy doped with pentaerythritol ethoxylate (PEE) and 2-naphthalene sulfonate (2-NS-PPy) separately via electropolymerization. Gold nanoparticles (AuNPs) were fixed on the PPy composite film by electrodeposition and then connected to CEA aptamer through self-assembly to construct a free-standing electrochemical biosensor breaking away from additional soft substrates and current collector. This PPy composite film-based electrochemical biosensor exhibits satisfying sensing performance for CEA detection, with a linear range from 10^{-10} g/mL to 10^{-6} g/mL and a detection limit of 0.033 ng/mL, good specificity and long-term sensing stability (96.8% of the original signal after 15 days). The biosensor also presents acceptable reproducibility with 1.7% relative standard deviation. Moreover, this electrochemical biosensor owns the deformation stability that could bear various deformations (twisting, folding, and knotting) without affecting device's sensing performance. It can even maintain 99.4% of the original signal under 25% strain deformation. Due to the superior sensing performance, high stability (mechanical deformation and long-term storage), and flexibility, this free-standing electrochemical biosensor proves huge potential in application of flexible and wearable electronics.

Keywords Flexible electrochemical biosensor · Free-standing · Polypyrrole · CEA · Non-faradaic electrochemical impedance

Introduction

Flexible sensors have been widely designed to monitor people's health in real-time, which could provide users health-related information and strengthen the management of chronic diseases [1]. The physical signals of the body (heartbeat, pulse, temperature, pressure) have been captured and converted into electrical signals based on flexible sensors [2–4]. Apart from the physical signals, disease biomarkers and biomolecules in biological fluids (such as sweat, saliva, and tears) and blood can be used as markers for certain diseases [5–7]. Until now, various methods for detecting biomarkers and biomolecules have been reported, such as enzyme-linked ImmunoSorbent Assay [8], photothermal immunoassay [9], surface-enhanced Raman spectroscopy [10, 11], fluorescence [12, 13], chemiluminescence immunoassay [14], and electrochemistry [15–17]. Among them, the electrochemical method is widely concerned by virtue of its simple operation, high sensitivity, and fast response [18]. However, traditional electrochemical sensors are modified and constructed based on rigid electrodes such as glassy carbon electrode and gold electrode, which could not satisfy the need for flexibility and limits the development of flexible electrochemical sensors.

To obtain flexibility and wearability, flexible electrochemical sensors reported now to detect molecular markers in biological fluids and blood are mainly designed by incorporating sensor electrodes into soft substrates such as flexible polymer and wearable materials (gloves, glasses, and clothes) [19–22].

✉ Fengxian Gao
fengxian@mail.ustc.edu.cn

✉ Xiliang Luo
xiliangluo@qust.edu.cn

[1] Key Laboratory of Optic-electric Sensing and Analytical Chemistry for Life Science, MOE, Shandong Key Laboratory of Biochemical Analysis, Key Laboratory of Analytical Chemistry for Life Science in Universities of Shandong, College of Chemistry and Molecular Engineering, Qingdao University of Science and Technology, Qingdao 266042, China

For example, a flexible sensor platform based on nitrile gloves was reported to in situ detect electrolytes and small molecule biomarkers in sweat. The sensing platform is suitable for versatile health and physiological real-time monitoring applications in daily life [23]. In addition, an entirely laser-engraved sensor based on polyimide substrate with simultaneous sweat collecting, chemical sensing, and vital signs monitoring was constructed [24]. The wearable sensor system can detect uric acid (UA) and tyrosine (Tyr) in sweat which is correlated with the concentration in blood and is expected to be used for personalized detection. These flexible electrochemical sensors are combined with soft substrates as well as additional current collector. The integration and the designing processes are complicated. Moreover, the modulus among sensor electrode materials, soft substrates, and current collector are quite different, which would cause delamination of the sensor's different parts under repeated usage and mechanical deformation. Thus, these flexible electrochemical sensors provide weak durability and low stability. Aiming to improve the stability and flexibility, electrochemical sensors based on flexible free-standing electrodes breaking away from additional soft substrates and current collector are quite required.

Researchers have tried to design flexible free-standing electrodes for flexible electrochemical sensors. A flexible free-standing aptamer sensor based on a flexible three-dimensional carbon nano-mesh was prepared to detect carcinogenic biomarkers (platelet-induced growth factors) [25]. Free-standing paper electrode based on graphene/Ag nanoparticles/poly(pyronin Y) was also prepared for the detection of nitrite [26]. However, these free-standing electrochemical sensors perform poor mechanical performance and low flexibility in spite of high sensitivity.

To overcome the problems talked above, we have designed a flexible free-standing electrochemical biosensor to detect carcinoembryonic antigen (CEA) based on conducting polypyrrole (PPy) composite film electrode. CEA, representing a typical tumor marker, has attracted wide attention in application of the early clinical detection of malignant tumors, and possesses important clinical value in differential diagnosis, disease monitoring, and efficacy evaluation [9, 27, 28]. In our previous work, we have synthesized PPy doped with pentaerythritol ethoxylate (PEE) (referred as PEE-PPy) mimicking animal dermis' dynamic network [29]. PEE-PPy performs superior mechanical performance and high conductivity, exhibiting giant potential as flexible electronic materials. Herein, we synthesize a flexible free-standing PPy composite film with sandwiched structure by combination of PEE-PPy and PPy doped with 2-naphthalene sulfonate (referred as 2-NS-PPy). 2-NS-PPy was directly polymerized on the two surfaces of PEE-PPy. According to our previous report, 2-NS-PPy could improve the PPy composite film's conductivity stability [30]. After that, gold nanoparticles (AuNPs) were modified on the thin composite film by electrochemical deposition, and the CEA aptamer is modified to the electrode surface through the self-assembly of the interaction between Au and sulfhydryl group. 6-Mercapto-1-hexanol (MCH) was finally used as blocking agent to block the remaining active sites to establish a flexible film electrode. Without need for additional soft substrate and current collector, this aptamer-functionalized film electrode can be directly used to fabricate a flexible free-standing electrochemical biosensor for CEA detection. The biosensor's specificity, sensitivity, reproducibility, stability, and flexibility were investigated.

Experimental section

Chemicals and reagents

Isopropanol (99%), $HAuCl_4$, and KNO_3 (99%) were provided by Sinopharm Chemical Reagent Co., Ltd. (Beijing, China). Tetra-armed PEG (pentaerythritol ethoxylate, referred as PEE, Mn ~ 800), boron trifluoride diethyl etherate (BFEE, 47%), 6-mercapto-1-hexanol (MCH), and pyrrole (99%) were purchased from Sigma-Aldrich. Sodium 2-naphthalenesulfonate, 2-naphthalenesulfonic acid, and triton X-100 were provided by Aladdin (Shanghai, China). Carcinoembryonic antigen (CEA), myoglobin (MB), lysozyme (Lys), and bovine serum albumin (BSA) were obtained from Beijing Boyanghongda Biological Technology Co., Ltd. (Beijing, China). The functional CEA aptamer was synthesized from Sangon Biotech Co., Ltd. (Shanghai, China) and the sequence was as follows: 5′-SH-ATA CCA GCT TAT TCA ATT-3′. Human immunoglobulin G (IgG) lyophilized powder was obtained from Equitech-Bio (Kerrville, TX). The reagents used in the experiment were all analytical grade. Pyrrole and BFEE were distilled under reduced pressure prior to use. Deionized water purified by a Milli-Q water purification system was used in this experiment.

Instrumentation

Scanning electron microscopy (SEM) was characterized with a JEOL JSM-7500F field emission electron microscopy (Hitachi High-Technology Co. Ltd., Japan). All electrochemical characterizations were carried out at a CHI 660E electrochemical workstation (Shanghai Chenhua Instrument Co. Ltd., China). The mechanical properties of PPy composite films were tested by INSTRON 3343 universal testing instrument at room temperature. The width of the sample was 0.4 cm and the length was 3 cm. The distance between the upper and lower clamps on the INSTRON machine was 6 mm. The elongation rate was 1 mm/min.

Preparation of the PPy composite film with sandwiched structure

PEE-PPy was synthesized through electropolymerization referring to previous report [29]. By controlling the polymerization time, thickness of the PEE-PPy film was fixed at 15 μm. The PPy composite film with sandwiched structure was synthesized according to our previous report [30]. By virtue of PEE-PPy film's good conductivity, 2-NS-PPy was synthesized on PEE-PPy film's surface with the PEE-PPy film directly acting as working electrode. Detailed procedure was provided in the supplementary information. Finally, a free-standing PPy composite film with sandwiched structure was obtained.

Construction of the free-standing electrochemical biosensor

The construction process of the electrochemical biosensor was shown in Scheme 1. The preparation of the electrochemical biosensor adopted a three-electrode system consisting of a platinum wire as the counter electrode, the PPy composite film with sandwiched structure as the working electrode and a saturated calomel electrode (SCE) as the reference electrode. The preparation process was conducted on the CHI 660E workstation. The PPy composite film was directly connected to the CHI 660E workstation through an alligator clip. The area of the membrane electrode was controlled at 4 mm × 4 mm. AuNPs were electrodeposited onto the surface of PPy composite film with the deposition potential of − 0.4 V in a 0.5 mM $HAuCl_4$ aqueous solution containing 0.5 M KNO_3 for 400 s. The AuNPs/PPy composite film was then immersed in 2 μM CEA aptamer solution overnight to modify the functionalized aptamer through self-assembly. After that, the membrane electrode was soaked in 1 mM MCH for 1 h to seal the remaining active sites. Finally, a free-standing MCH/aptamer/AuNPs/PPy composite film-based electrochemical biosensor was successfully fabricated. For CEA detection, the aptamer-functionalized film electrode was soaked in CEA solutions of various concentrations for 60 min. All operation steps were carried out at room temperature.

Electrochemical characterization of the free-standing electrochemical biosensor

Performance of the electrochemical biosensor was evaluated by non-faradaic electrochemical impedance spectroscopy (EIS) test on the CHI 660E workstation in PBS (0.2 M, pH 7.4) solution with the frequency range from 0.1 to 100,000 Hz, the amplitude of 5 mV, and the applied voltage of 0.0 V. The test adopted three-electrode system in which the aptamer-modified PPy composite film, the saturated calomel electrode (SCE) and the platinum wire were used as the working electrode, the reference electrode and the counter electrode, respectively. All EIS tests were carried out at room temperature and the data was collected at 10 Hz.

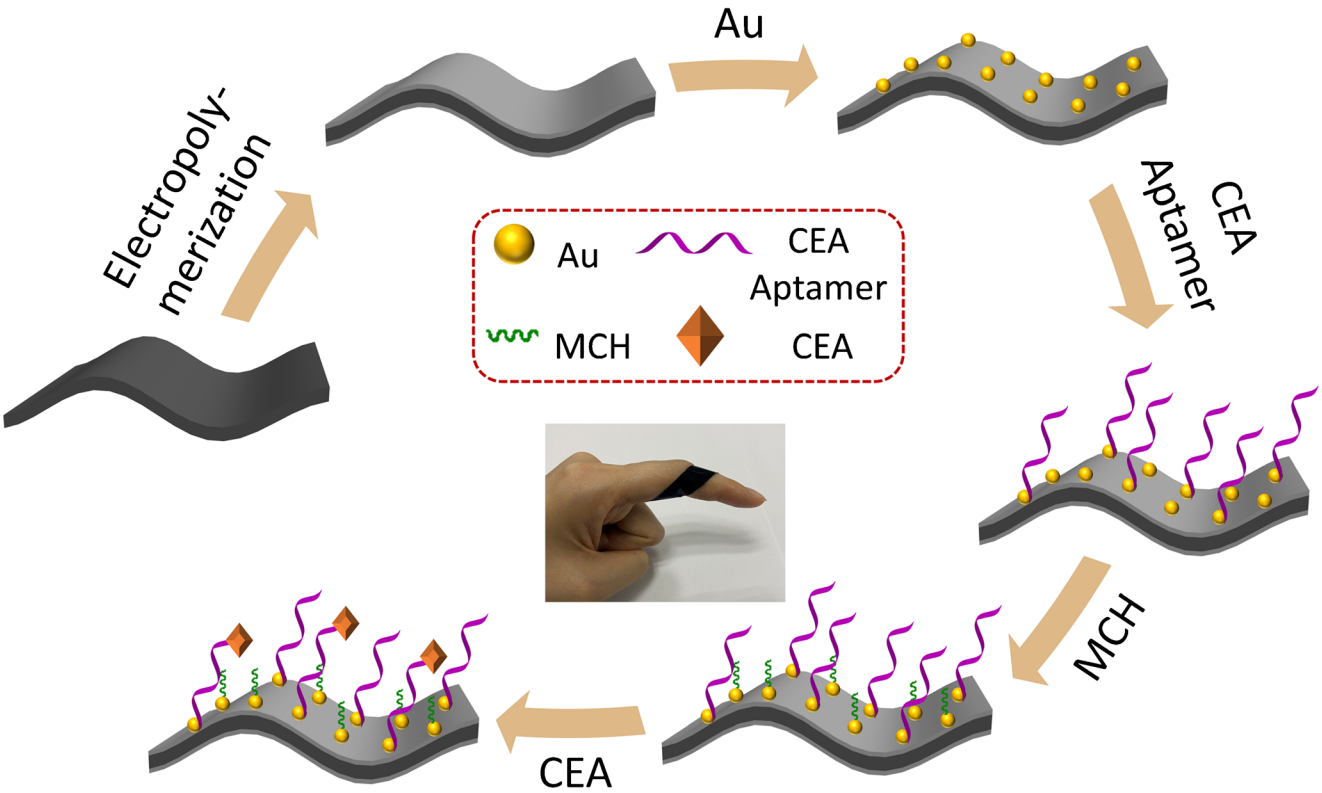

Scheme 1 Schematic diagram of the construction process of the free-standing electrochemical biosensor based on PPy composite film

Results and discussion

Characterization of the electrochemical biosensor construction process

The microscopic morphology of the PPy composite film and AuNPs/PPy composite film electrode were characterized by SEM. The PPy composite film presents cauliflower-like structure (Fig. S1). Taking advantage of PPy composite film's free-standing and conductive characteristics, AuNPs were modified on its surface via electrodeposition by directly using the PPy composite film as working electrode. Figure 1a shows that AuNPs were uniformly dispersed on the film surface with an average particle size of 170–670 nm, indicating the successful electrodeposition. Non-faradaic EIS test was adopted to characterize the successful fabrication of the electrochemical biosensor (Fig. 1b). Compared to the PPy composite film, the baseline impedance significantly decreased after introducing AuNPs onto the film. The AuNPs facilitate the electron transfer speed of the sensing interface. The AuNPs/PPy composite film was then subjected to CEA aptamer (containing sulfhydryl group). As shown in Fig. 1b, the impedance value increased significantly. This can be ascribed to the self-assembly of the functionalized CEA aptamer and AuNPs through the interaction between Au and sulfhydryl group. Due to the poor conductivity of the aptamer, the impedance increased accordingly. AuNPs on the PPy composite film that were not bound to the aptamer would affect the aptamer sensor. In order to prevent non-specific adsorption and maintain the recognition ability of the biosensor, MCH was used to block the remaining activation sites. Figure 1b shows that the impedance increased, which results from MCH's blocking effect [31, 32]. After incubating with the target detection substance CEA, the baseline impedance of the biosensor further increased due to the stereo-hindrance effect and non-conductivity of CEA. The changes about impedance value on each step prove that the electrochemical biosensor has been successfully fabricated, and the signal change after being combined with the target confirms the feasibility of the biosensor.

Optimization of experimental conditions for the electrochemical biosensor

Aim to maximize the sensing performance of the free-standing electrochemical biosensor, the polymerization time of 2-NS-PPy on PEE-PPy and the electrodeposition conditions of AuNPs, aptamer concentration and the CEA incubation time were discussed and optimized, respectively. Fig. S2 presents that the impedance signal change firstly increased and then declined, and reached the maximum when the polymerization time of 2-NS-PPy was 20 min. Thus, 20 min was selected as the optimal polymerization time for the 2-NS-PPy layer. The deposition voltage was investigated from − 0.6 V to − 0.2 V, and the highest impedance change was observed at − 0.4 V (Fig. S3a). By changing the deposition time, the impedance signal change reached the maximum when the deposition time was 400 s (Fig. S3b). Consequently, − 0.4 V and 400 s were employed as the most suitable conditions for the electrodeposition of AuNPs. The aptamer concentration and the incubation time of CEA were then optimized. As the concentration of aptamer increased, the impedance change continued to increase and reached nearly stable at 2.0 μM (Fig. 2a). For the sake of obtaining the optimal CEA incubation time, the aptamer-modified thin-film biosensor was soaked in 0.2 M

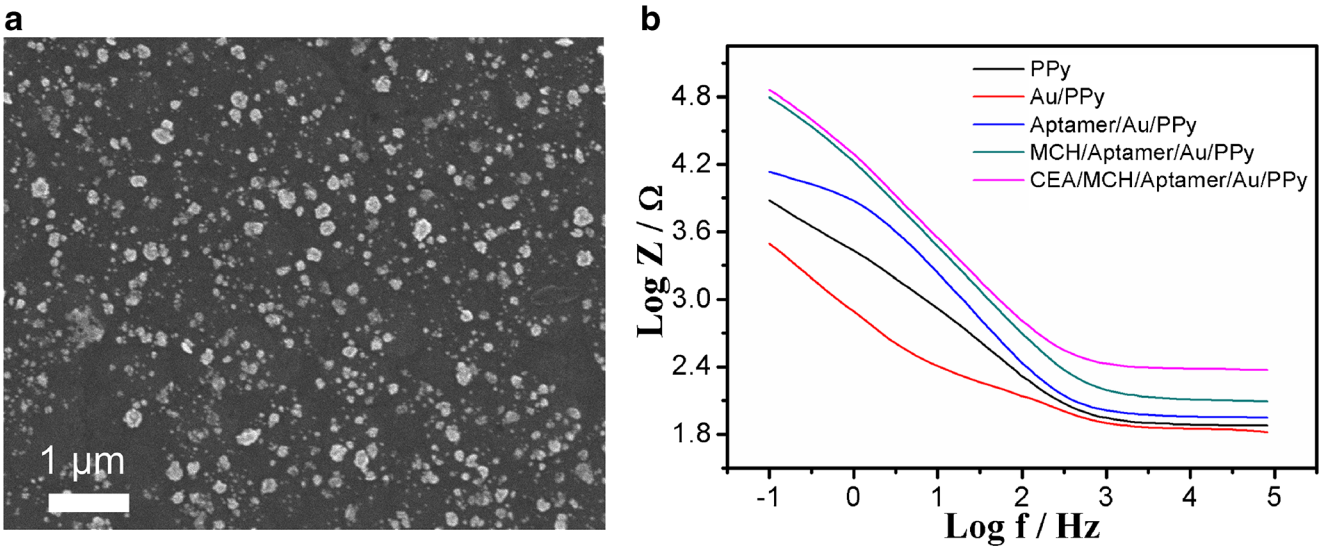

Fig. 1 Morphology characterization and feasibility of the electrochemical biosensor construction process. **a** SEM of the AuNPs/PPy composite film. **b** The non-faradaic EIS curves of different modified electrodes in PBS solution (0.2 M, pH 7.4)

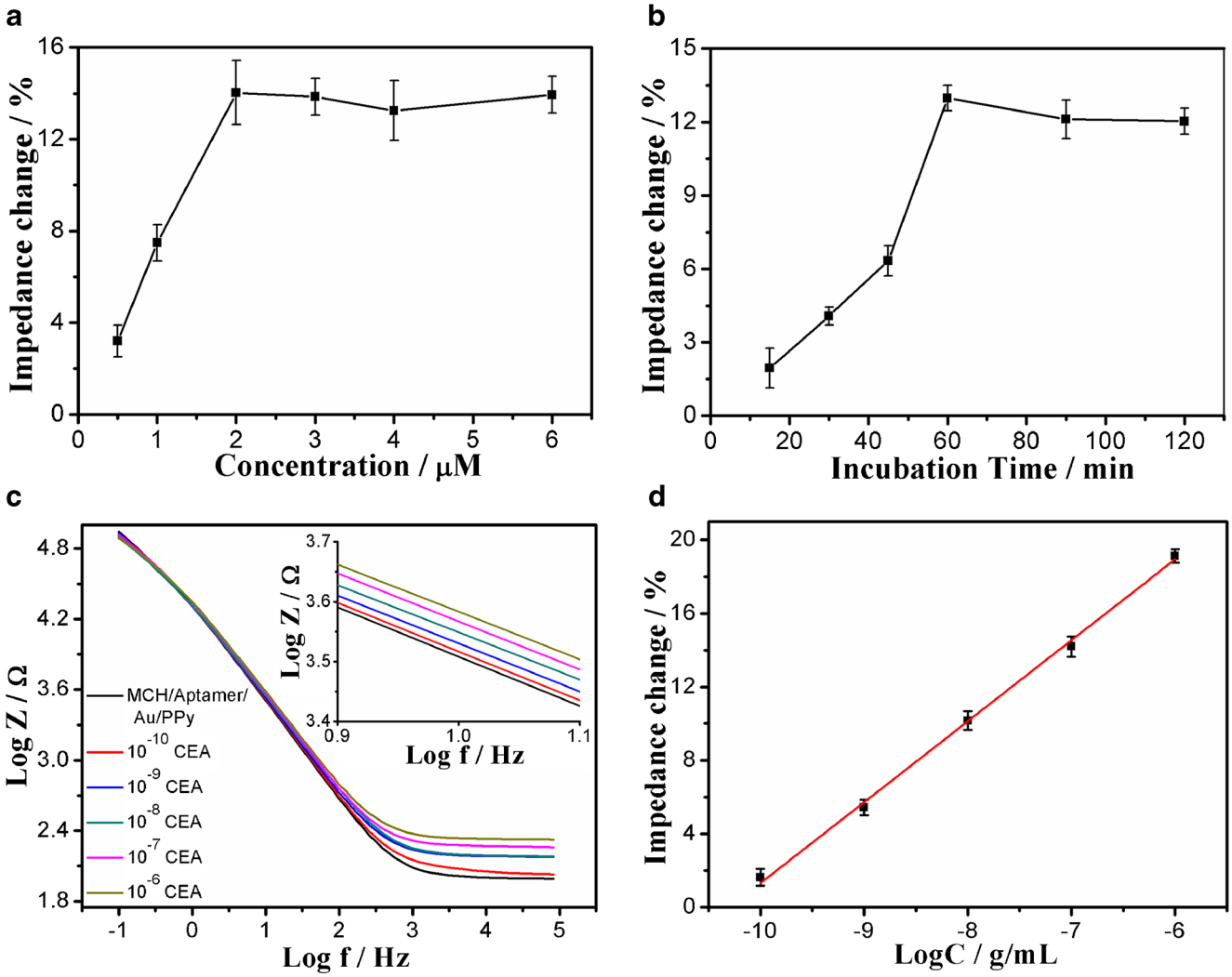

Fig. 2 Optimization of experimental conditions and electrochemical detection of CEA. The non-faradaic EIS tests were performed in PBS (0.2 M, pH 7.4). **a** Effects of the aptamer concentration on the non-faradaic impedance responses of the biosensor. **b** Effects of the CEA incubation time on the non-faradaic impedance responses of the biosensor. **c** The non-faradaic curves of the biosensor after incubation with different concentrations of CEA. The internal inset is a partial enlarged view with an impedance frequency of 10 Hz. **d** The linear calibration curve about the non-faradaic impedance change and the logarithm of CEA concentration. Error bars represent the standard deviations of three repeated determinations ($n = 3$)

PBS (pH 7.4) solution containing 10^{-6} g/mL CEA for different times, and the EIS values were measured separately (Fig. 2b). Figure 2b shows that the impedance signal change of the biosensor increased as the incubation time extended and kept almost equilibrium at 60 min. This indicates that the binding of CEA and aptamer has attained saturation. According to the experimental results, the aptamer concentration of 2.0 μM and the CEA incubation time of 60 min were chosen as optimal experimental conditions for the electrochemical biosensor.

Electrochemical detection of CEA

The sensing performance of the free-standing electrochemical biosensor was characterized by performing non-faradaic EIS tests in 0.2 M PBS (pH 7.4) solution (Fig. 2c). Figure 2c and d shows that there was a linear relationship between the change of impedance signal and the logarithm of CEA concentration, with the concentration ranging from 0.1 ng/mL to 1 μg/mL. The linear equation is $\Delta R/R_0 = 45.27 + 4.41$ logC ($R^2 = 0.9980$), and the detection limit of this biosensor is calculated to be 0.033 ng/mL ($S/N = 3$). Most of the electrochemical biosensors constructed for CEA detection are not flexible and they need to be integrated with rigid electrodes. Compared with the traditional electrochemical biosensors referred in Table S1, our free-standing electrochemical biosensor based on conducting PPy composite film electrode exhibits comparable sensing performance.

Specificity, stability, reproducibility, and practical application of the electrochemical biosensor

The specific detection of the electrochemical biosensor to target CEA was evaluated by choosing some representative proteins as possible interferences, such as bovine serum albumin (BSA), myoglobin (MB), lysozyme (Lys), and human immunoglobulin G (IgG). Compared with the other four interfering proteins (BSA, MB, Lys, IgG), this electrochemical biosensor only presents significant impedance signal change to CEA and the mixed solution containing CEA. The result indicates that this biosensor enables to detect CEA effectively in the presence of other interferences (Fig. 3a).

Fig. 4 Characterization of the deformability of the electrochemical biosensor. The non-faradaic EIS tests were performed in PBS (0.2 M, pH 7.4) solution. **a** Photographs of the aptamer-functionalized PPy composite film electrode. **b** The stress-strain curve of the PPy composite film. **c**–**e** The non-faradaic EIS curves of the CEA-incubated biosensor before and after various deformation (twisting, folding, and knotting). **f** Comparison of the non-faradaic impedance signal change of the CEA-incubated biosensor before and after mechanical deformation. **g** The impedance retention of the biosensor under different strain

In order to measure the long-term storage stability of the biosensor, the aptamer-modified PPy film electrodes were immersed in PBS solution and stored in the air for 15 days, respectively. The impedance retention was tested through

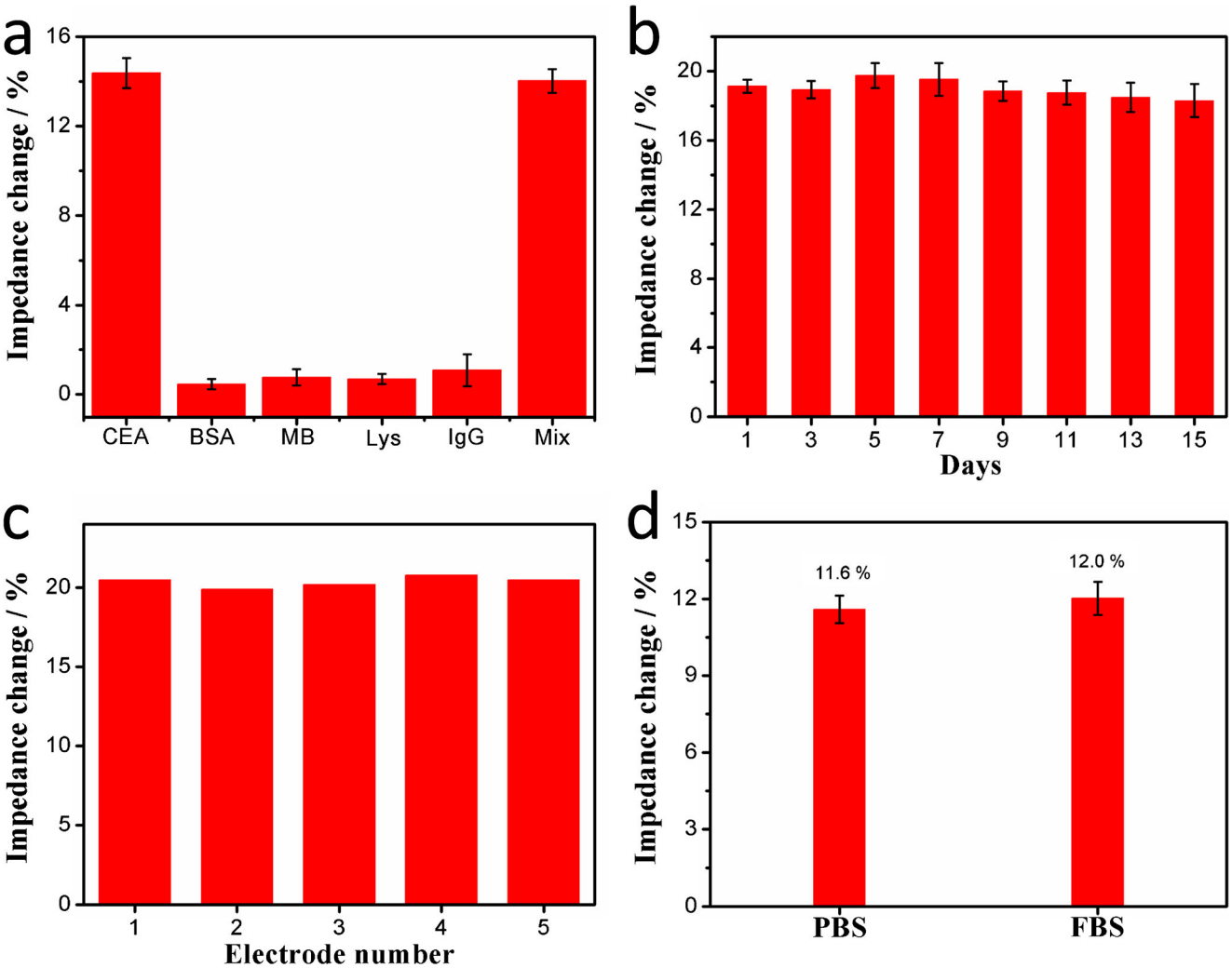

Fig. 3 Characterization of the electrochemical biosensor's specificity, stability, reproducibility, and practical application. The non-faradaic EIS tests were performed in PBS (0.2 M, pH 7.4) solution. **a** The non-faradaic impedance response change of the biosensor to 10^{-7} g/mL of CEA, BSA, MB, Lys, and IgG, and the mixture (Mix) containing CEA with all the other four proteins, respectively. **b** The long-term sensing stability of the biosensor for CEA detection stored in PBS (0.2 M, pH 7.4) for 15 days. **c** The signal response of five independent electrodes to 10^{-6} g/mL CEA. **d** Comparison of the non-faradaic impedance signal change of the biosensor in PBS and FBS. The biosensor was incubated with 10^{-8} g/mL CEA in PBS and FBS solution, respectively

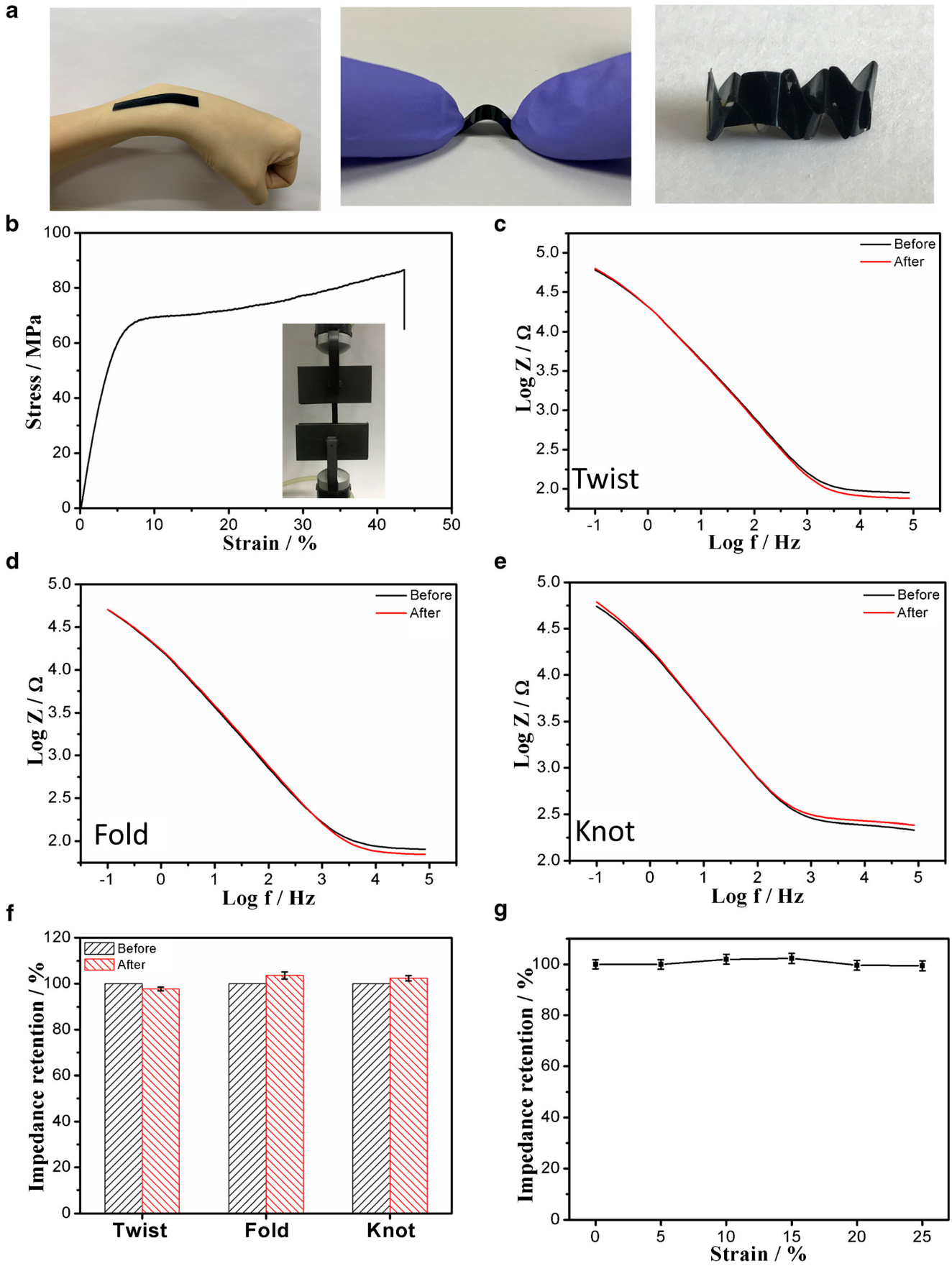
a
b
Stress / MPa
Strain / %
c
Before
After
Log Z / Ω
Log f / Hz
Twist
d
Fold
e
Knot
f
Impedance retention / %
Twist
Fold
Knot
g
Impedance retention / %
Strain / %

non-faradaic EIS test. Fig. S4 shows that the impedance kept nearly no change no whether immersed in PBS or stored in the air. The aptamer-functionalized biosensors were also immersed in 0.2 M PBS for 15 days and were used to detect CEA (10^{-6} g/mL) every 2 days. Figure 3b demonstrates that the impedance signal change only dropped 3.2%. These results prove that the electrochemical biosensor designed has the capacity to support long-term CEA sensitive detection.

Reproducibility is a key parameter to evaluate the performance of a biosensor. In this work, five independently prepared CEA electrochemical biosensors were used to detect CEA (10^{-6} g/mL) under the same experimental condition. As shown in Fig. 3c, no significant difference of the impedance change was observed among the five electrodes and the relative standard deviation (RSD) was calculated to be 1.7%, which proves the biosensor's acceptable reproducibility.

In addition, we tested the feasibility of the electrochemical biosensor for practical application by simulating a complex biological environment with fetal bovine serum (FBS) in this experiment (as shown in Fig. 3d). The FBS solution and PBS solution both containing CEA (10^{-8} g/mL) were detected by the PPy composite film-based electrochemical biosensor respectively. The impedance change measured in FBS solution is basically the same as that measured in PBS, indicating the biosensor's potential for real application.

Flexibility and mechanical deformation stability of the free-standing electrochemical biosensor

The PPy composite film exhibits excellent mechanical property with the tensile strength of 86.6 MPa, the elongation-at-break of 43.7%, and the Young's modulus of 0.72 GPa (Fig. 4b). Owing to the film's superior mechanical property, the aptamer-functionalized PPy composite film electrode also presents the deformability, which can be made into various shapes and models (Fig. 4a). The film electrode has a good fit to the skin and can be bended or even folded into the spring-like model. In order to investigate the biosensor's flexibility, the impedance signal was recorded before and after deformation. Fig. S5 shows that the impedance signal of the biosensor remained more than 95% of the original signal after a series of mechanical deformations (twisting, folding, and knotting). The effect of mechanical deformation on the impedance signal of the biosensor which has been incubated with CEA was discussed (Fig. 4c–f). As shown in Fig. 4c–e, the non-faradaic EIS curves of the CEA-incubated biosensor before and after deformation almost coincide with each other. The impedance change recorded at the frequency of 10 Hz was within 5% after deformation (Fig. 4f). Therefore, the deformations perform nearly no effect on its electrochemical sensing performance. The impedance retention of the electrochemical biosensor under different strain was also tested accordingly. Figure 4g shows that the stretchability has almost no effect on the impedance signal of the biosensor, and it can maintain 99.4% of the unstretched signal under the strain of 25%. All these results prove that our biosensor performs certain mechanical deformation stability and flexibility. For the PPy composite film, the elongation-at-break is 43.7%, which limits the biosensor's stretchability. However, the biosensor could bear normal human body activities in the application of flexible electrochemical biosensors and have certain development space in flexible and wearable electronics.

Conclusions

This study describes a flexible free-standing electrochemical biosensor to detect CEA based on conducting PPy nanocomposite film electrode. The introduction of AuNPs can modify the aptamer to the electrode surface through self-assembly and MCH was used as block reagent to maintain the biosensor's good recognition ability. This free-standing biosensor exhibits satisfying sensitivity, selectivity, reproducibility, and long-term stability. Moreover, this PPy composite film-based electrochemical biosensor possesses high mechanical deformation stability and flexibility. It could bear various deformations without affecting the sensor's performance. The free-standing biosensor platform we constructed performs huge space for development in the field of flexible and wearable electronics. The way we constructed the flexible free-standing film electrode based on conducting polymer provides new ways for designing flexible electrochemical biosensors.

Supplementary Information The online version contains supplementary material available at https://doi.org/10.1007/s00604-021-04859-1.

Funding This work was supported by Natural Science Foundation of Shandong Province (ZR2019BB008), National Natural Science Foundation of China (21974075), Talent Fund of Shandong Collaborative Innovation Center of Eco-Chemical Engineering (XTCXQN09), the Taishan Scholar Program of Shandong Province of China (ts20110829), and the Science and Technology Benefiting the People Project of Qingdao (20-3-4-53-nsh).

Declarations

Conflict of interest The authors declare no competing interests.

References

1. Kim J, Campbell AS, de Ávila BE-F, Wang J (2019) Wearable biosensors for healthcare monitoring. Nat Biotechnol 37(4):389–406
2. Hong YJ, Jeong H, Cho KW, Lu N, Kim DH (2019) Wearable and implantable devices for cardiovascular healthcare: from monitoring to therapy based on flexible and stretchable electronics. Adv Funct Mater 29(19):1808247

3. Zhang K, Sun J, Song J, Gao C, Wang Z, Song C, Wu Y, Liu Y (2020) Self-healing Ti_3C_2 MXene/PDMS supramolecular elastomers based on small biomolecules modification for wearable sensors. ACS Appl Mater Interfaces 12(40):45306–45314
4. Nie K, Wang Z, Tang R, Zheng L, Li C, Shen X, Sun Q (2020) Anisotropic, flexible wood hydrogels and wrinkled, electrodeposited film electrodes for highly sensitive, wide-range pressure sensing. ACS Appl Mater Interfaces 12(38):43024–43031
5. Kim J, Sempionatto JR, Imani S, Hartel MC, Barfidokht A, Tang GD, Campbell AS, Mercier PP, Wang J (2018) Simultaneous monitoring of sweat and interstitial fluid using a single wearable biosensor platform. Adv Sci 5(10):1800880
6. Lei Y, Zhao W, Zhang Y, Jiang Q, He JH, Baeumner AJ, Wolfbeis OS, Wang ZL, Salama KN, Alshareef HN (2019) A MXene-based wearable biosensor system for high-performance in vitro perspiration analysis. Small 15(19):1901190
7. Vargas E, Teymourian H, Tehrani F, Eksin E, Sánchez-Tirado E, Warren P, Erdem A, Dassau E, Wang J (2019) Enzymatic/immunoassay dual-biomarker sensing chip: towards decentralized insulin/glucose detection. Angew Chem Int Ed 58(19):6376–6379
8. Jiao L, Yan H, Xu W, Wu Y, Gu W, Li H, Du D, Lin Y, Zhu C (2019) Self-assembly of all-inclusive allochroic nanoparticles for the improved ELISA. Anal Chem 91(13):8461–8465
9. Zhang B, Hu X, Jia Y, Li J, Zhao Z (2021) Polyaniline@Au organic-inorganic nanohybrids with thermometer readout for photothermal immunoassay of tumor marker. Microchim Acta 188(3):63
10. Achadu OJ, Abe F, Suzuki T, Park EY (2020) Molybdenum trioxide nanocubes aligned on a graphene oxide substrate for the detection of nrovirus by surface-enhanced raman scattering. ACS Appl Mater Interfaces 12(39):43522–43534
11. Gholami MD, Sonar P, Ayoko GA, Izake EL (2020) A highly sensitive SERS quenching nanosensor for the determination of tumor necrosis factor alpha in blood. Sens Actuators B: Chem 310:127867
12. Hou L, Qin Y, Li J, Qin S, Huang Y, Lin T, Guo L, Ye F, Zhao S (2019) A ratiometric multicolor fluorescence biosensor for visual detection of alkaline phosphatase activity via a smartphone. Biosens Bioelectron 143:111605
13. Xu S, Jiang L, Wang J, Gao Y, Luo X (2019) Ratiometric multicolor analysis of intracellular microRNA using a chain hybrid substitution-triggered self-assembly of silver nanocluster-based label-free sensing platform. ACS Appl Mater Interfaces 12(1):373–379
14. Yu L, Zhang Q, Kang Q, Zhang B, Shen D, Zou G (2020) Near-infrared electrochemiluminescence immunoassay with biocompatible Au nanoclusters as tags. Anal Chem 92(11):7581–7587
15. Xu Z, Teng H, Song J, Gao F, Ma L, Xu G, Luo X (2019) A nanocomposite consisting of MnO_2 nanoflowers and the conducting polymer PEDOT for highly sensitive amperometric detection of paracetamol. Microchim Acta 186(8):499
16. Liu N, Song J, Lu Y, Davis JJ, Gao F, Luo X (2019) Electrochemical aptasensor for ultralow fouling cancer cell quantification in complex biological media based on designed branched peptides. Anal Chem 91(13):8334–8340
17. Xu Z, Han R, Liu N, Gao F, Luo X (2020) Electrochemical biosensors for the detection of carcinoembryonic antigen with low fouling and high sensitivity based on copolymerized polydopamine and zwitterionic polymer. Sens Actuators B: Chem 319:128253
18. Zhou Y, Yin H, Zhao W-W, Ai S (2020) Electrochemical, electrochemiluminescent and photoelectrochemical bioanalysis of epigenetic modifiers: a comprehensive review. Coord Chem Rev 424:213519
19. Hui X, Sharifuzzaman M, Sharma S, Xuan X, Zhang S, Ko SG, Yoon SH, Park JY (2020) High-performance flexible electrochemical heavy metal sensor based on layer-by-layer assembly of $Ti_3C_2T_x$/MWNTs nanocomposites for noninvasive detection of copper and zinc ions in human biofluids. ACS Appl Mater Interfaces 12(43):48928–48937
20. Zhang Y, Lv Q, Chi K, Li Q, Fan H, Cai B, Xiao F, Wang S, Wang Z, Wang L (2021) Hierarchical porous carbon heterojunction flake arrays derived from metal organic frameworks and ionic liquid for H_2O_2 electrochemical detection in cancer tissue. Nano Res 14(5):1335–1343
21. Khoshroo A, Sadrjavadi K, Taran M, Fattahi A (2020) Electrochemical system designed on a copper tape platform as a nonenzymatic glucose sensor. Sens Actuators B: Chem 325:128778
22. Xu M, Obodo D, Yadavalli VK (2019) The design, fabrication, and applications of flexible biosensing devices. Biosens Bioelectron 124-125:96–114
23. Bariya M, Li L, Ghattamaneni R, Ahn CH, Nyein HYY, Tai L-C, Javey A (2020) Glove-based sensors for multimodal monitoring of natural sweat. Sci Adv 6(35):eabb8308
24. Yang Y, Song Y, Bo X, Min J, Pak OS, Zhu L, Wang M, Tu J, Kogan A, Zhang H, Hsiai TK, Li Z, Gao W (2019) A laser-engraved wearable sensor for sensitive detection of uric acid and tyrosine in sweat. Nat Biotechnol 38(2):217–224
25. Kim W, Lee JS, Jang J (2020) Aptamer-functionalized three-dimensional carbon nanowebs for ultrasensitive and free-standing PDGF biosensor. ACS Appl Mater Interfaces 12(18):20882–20890
26. Dağcı K, Alanyalıoğlu M (2016) Preparation of free-standing and flexible graphene/Ag nanoparticles/poly(pyronin Y) hybrid paper electrode for amperometric determination of nitrite. ACS Appl Mater Interfaces 8(4):2713–2722
27. Gu X, She Z, Ma T, Tian S, Kraatz H-B (2018) Electrochemical detection of carcinoembryonic antigen. Biosens Bioelectron 102:610–616
28. Wu Q, Li N, Wang Y, Xu Y, Wu J, Jia G, Ji F, Fang X, Chen F, Cui X (2020) Ultrasensitive and selective determination of carcinoembryonic antigen using multifunctional ultrathin amino-functionalized Ti_3C_2-MXene nanosheets. Anal Chem 92(4):3354–3360
29. Gao F, Zhang N, Fang X, Ma M (2017) Bioinspired design of strong, tough, and highly conductive polyol-polypyrrole composites for flexible electronics. ACS Appl Mater Interfaces 9(7):5692–5698
30. Gao F, Song J, Xu Z, Xu L, Guo Y, Miao L, Luo X (2021) All-polymer free-standing electrodes for flexible electrochemical sensors. Sens Actuators B: Chem 334:129675
31. Huang K-J, Liu Y-J, Zhang J-Z, Liu Y-M (2015) A sequence-specific DNA electrochemical sensor based on acetylene black incorporated two-dimensional CuS nanosheets and gold nanoparticles. Sens Actuators B: Chem 209:570–578
32. Zarei SS, Soleimanian-Zad S, Ensafi AA (2018) An impedimetric aptasensor for shigella dysenteriae using a gold nanoparticle-modified glassy carbon electrode. Microchim Acta 185(12):538